

Supporting Information

A trifunctional $\text{Co}_{0.85}\text{Se}/\text{NC}$ collaborated electrocatalyst enables a self-powered energy system for uninterrupted H_2 production

Wen-Wen Tian,^a Yi-Dai Ying,^a Jin-Tao Ren,^a and Zhong-Yong Yuan^{a,b,*}

^a *National Institute for Advanced Materials, School of Materials Science and Engineering, Nankai University, Tianjin 300350, China*

^b *Key Laboratory of Advanced Energy Materials Chemistry (Ministry of Education), Nankai University, Tianjin 300071, China*

* Corresponding author. E-mail address: zyyuan@nankai.edu.cn (Z.-Y. Yuan)

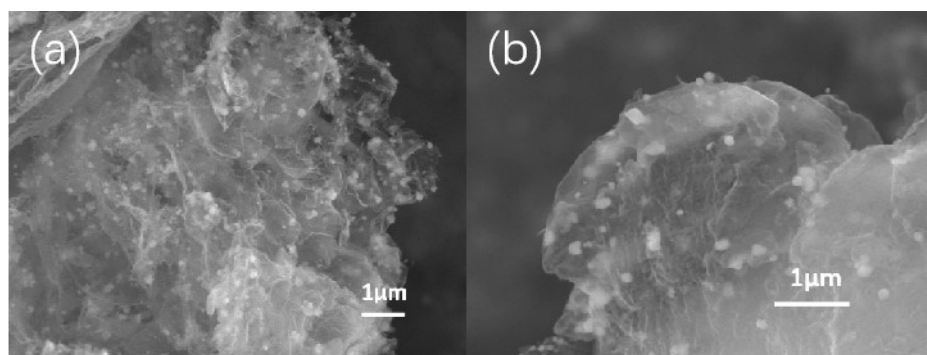


Fig. S1. SEM images of CoSe_2/NC .

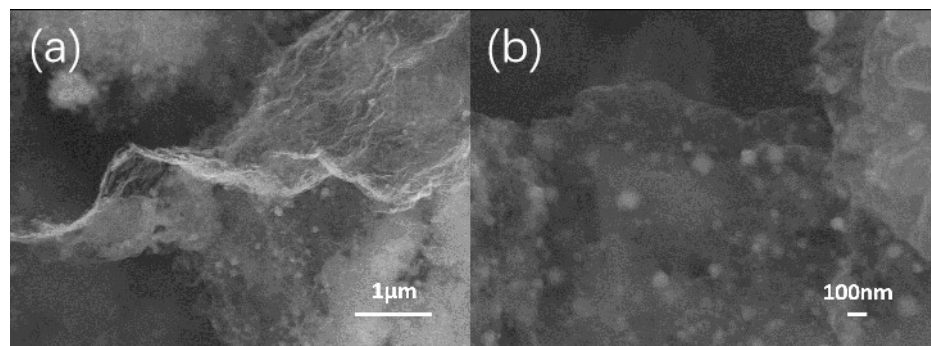


Fig. S2. SEM images of CoO/NC .

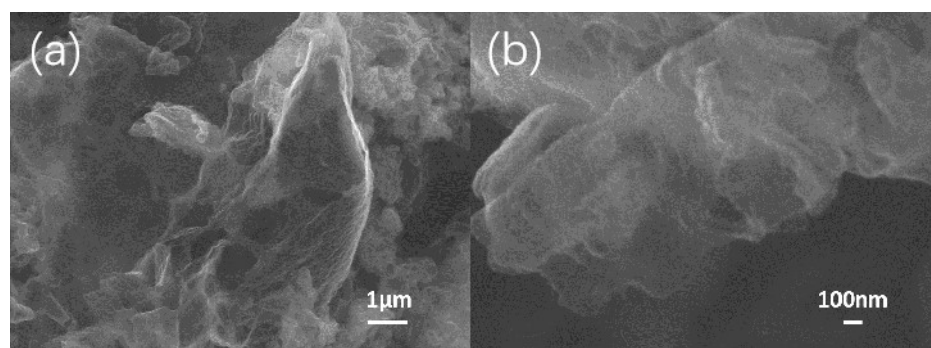


Fig. S3. SEM images of NC.

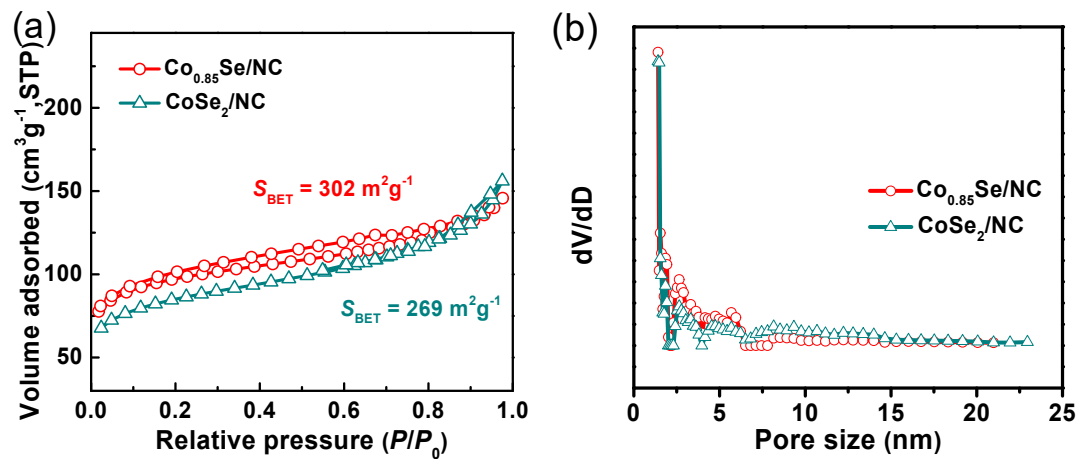


Fig. S4. N₂ adsorption-desorption isotherms and (b) pore size distribution curves of Co_{0.85}Se/NC and CoSe₂/NC catalysts.

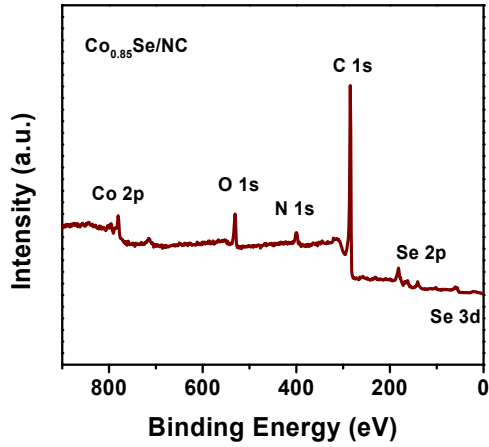


Fig. S5. XPS full spectra of Co_{0.85}Se/NC catalysts.

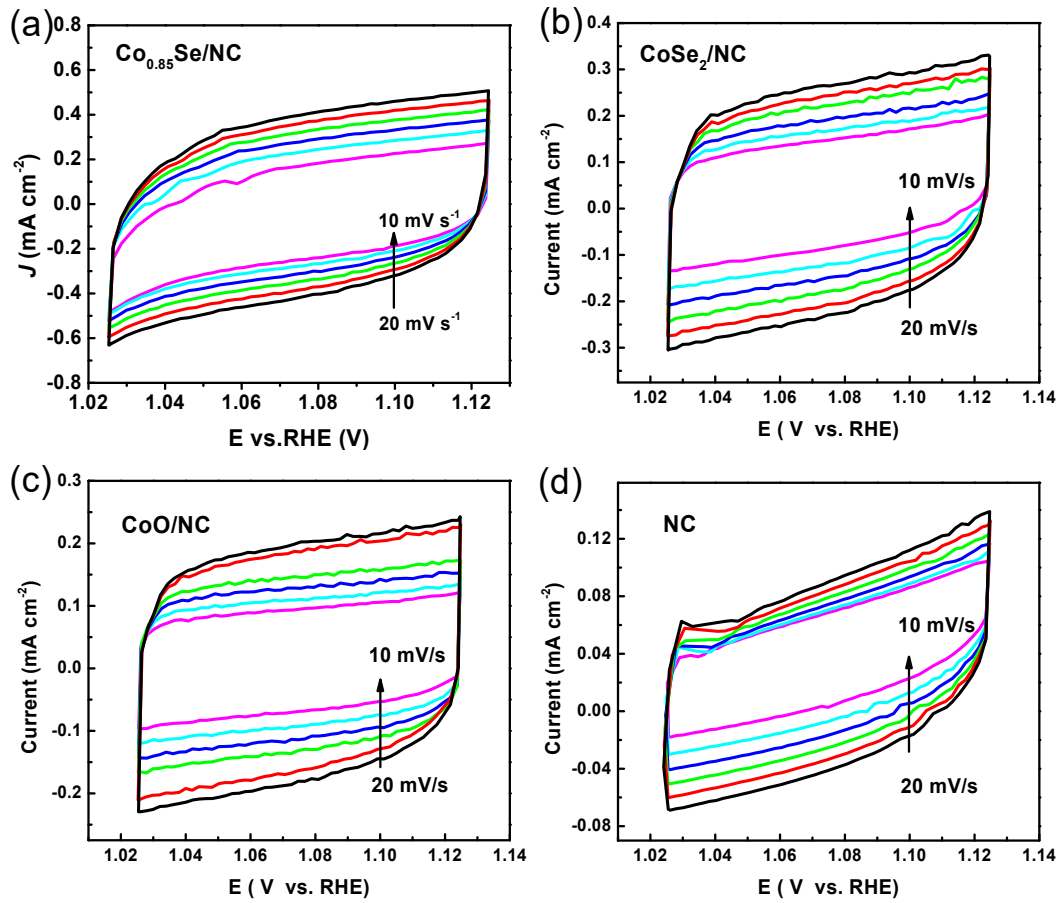


Fig. S6. CV curves at different scan rates from 10 to 20 mV s⁻¹ of different samples.

Calculation details of ECSA:

$$\text{ECSA} = C_{\text{dl}}/C_s$$

The electrical double layer capacitance (C_{dl}) values were calculated in terms of cyclic voltammetry (CV) curves at different scan rates from 10 to 20 mV s⁻¹. The electrochemically active surface area (ECSA) values were derived from the equation $\text{ECSA} = C_{\text{dl}}/C_s$, where C_s is the specific capacitance.[1] The C_s for a flat surface was in the range of 20-60 $\mu\text{F cm}^{-2}$,[2] and adopts the value of 60 $\mu\text{F cm}^{-2}$ here to roughly calculate the ECSA.

$$\text{ECSA}_{\text{Co}_{0.85}\text{Se}/\text{NC}} = 23.1 \text{ mF cm}^{-2} / 60 \mu\text{F cm}^{-2} = 385.0 \text{ cm}^{-2}_{\text{ECSA}}$$

$$\text{ECSA}_{\text{CoSe}_2/\text{NC}} = 12.5 \text{ mF cm}^{-2} / 60 \mu\text{F cm}^{-2} = 208.3 \text{ cm}^{-2}_{\text{ECSA}}$$

$$\text{ECSA}_{\text{CoO}/\text{NC}} = 11.6 \text{ mF cm}^{-2} / 60 \mu\text{F cm}^{-2} = 193.0 \text{ cm}^{-2}_{\text{ECSA}}$$

$$\text{ECSA}_{\text{NC}} = 2.7 \text{ mF cm}^{-2} / 60 \mu\text{F cm}^{-2} = 45.0 \text{ cm}^{-2}_{\text{ECSA}}$$

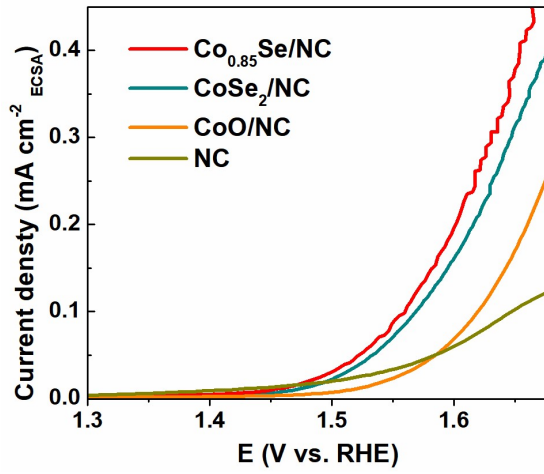


Fig. S7. OER activity of different catalysts in 1.0 M KOH normalized by ECSA.

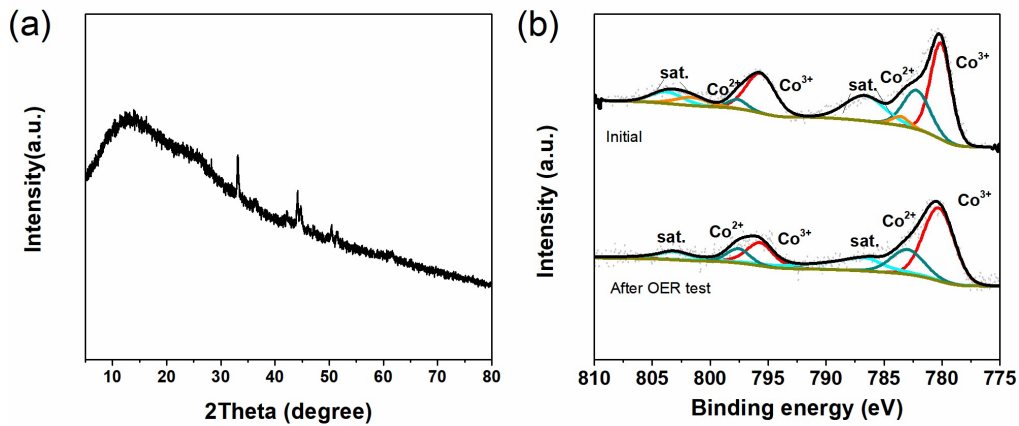


Fig. S8. (a) XRD pattern of $\text{Co}_{0.85}\text{Se}/\text{NC}$ after OER test. (b) Co 2p XPS high-resolution spectra of $\text{Co}_{0.85}\text{Se}/\text{NC}$ before and after OER test.

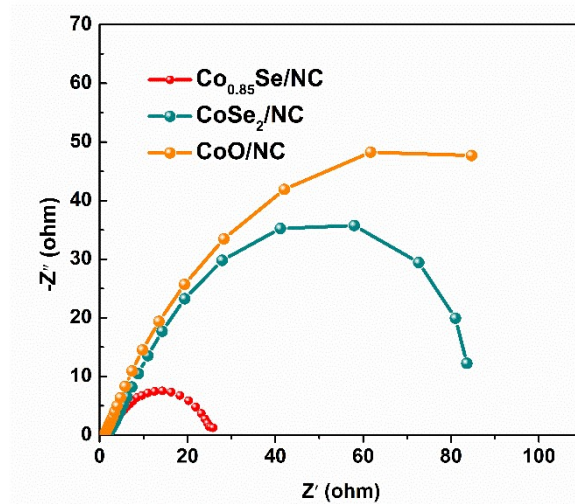


Fig. S9. Electrochemical impedance spectra of prepared catalysts during ORR process.

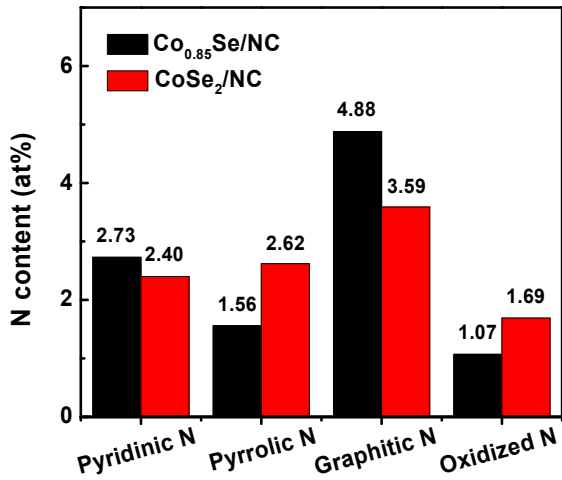


Fig. S10. The histogram refers to the content of different N types of Co_{0.85}Se/NC and CoSe₂/NC catalysts.

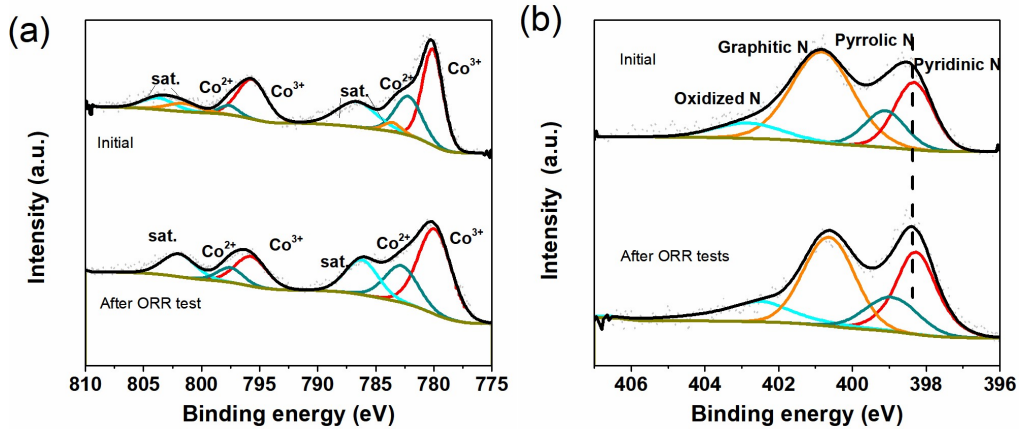


Fig. S11. (a) Co 2p and (b) N 1s XPS high-resolution spectra of Co_{0.85}Se/NC before and after ORR test.

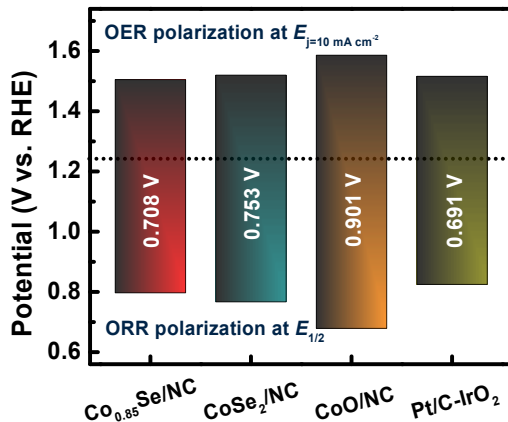


Fig. S12. The potential differences between the $E_{j=10}$ of OER and $E_{1/2}$ of ORR for different samples.

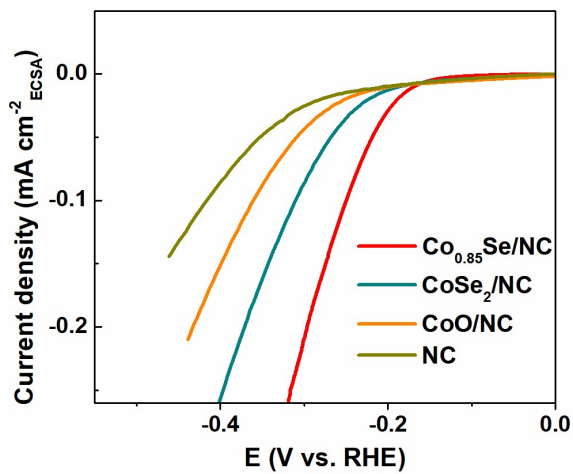


Fig. S13. HER activity of different catalysts in 1.0 M KOH normalized by ECSA.

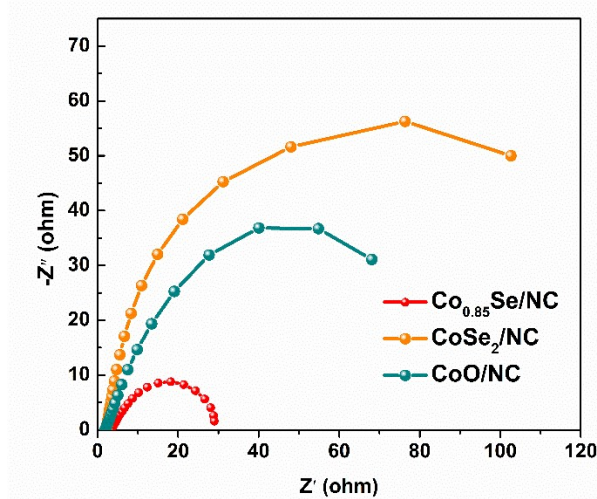


Fig. S14. Electrochemical impedance spectra of prepared catalysts during HER process.

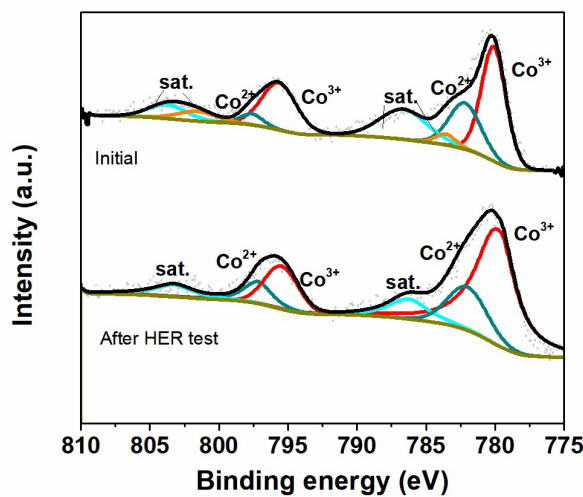


Fig. S15. Co 2p XPS high-resolution spectra of $\text{Co}_{0.85}\text{Se/NC}$ before and after HER test.

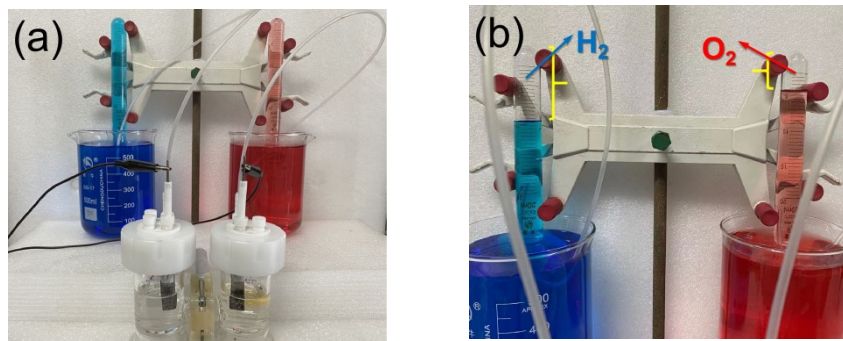


Fig. S16. The photographs of the water-gas displacing instrument.

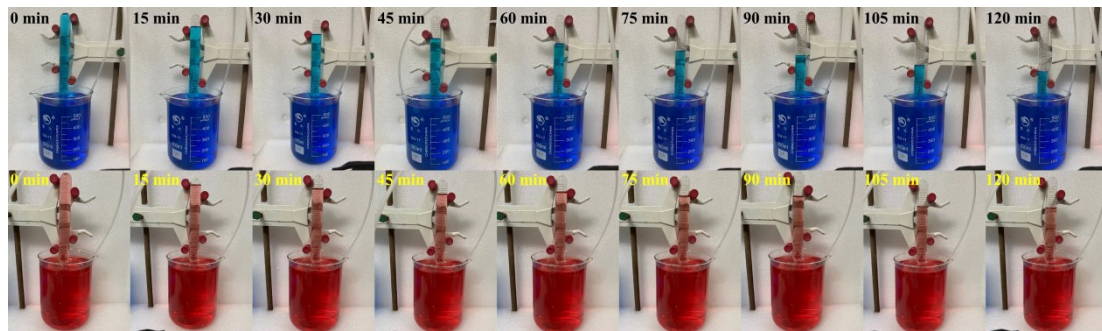


Fig. S17. The optical images of the gas collection tubes at fifteen-minute intervals over two-hour period during the overall water splitting process.

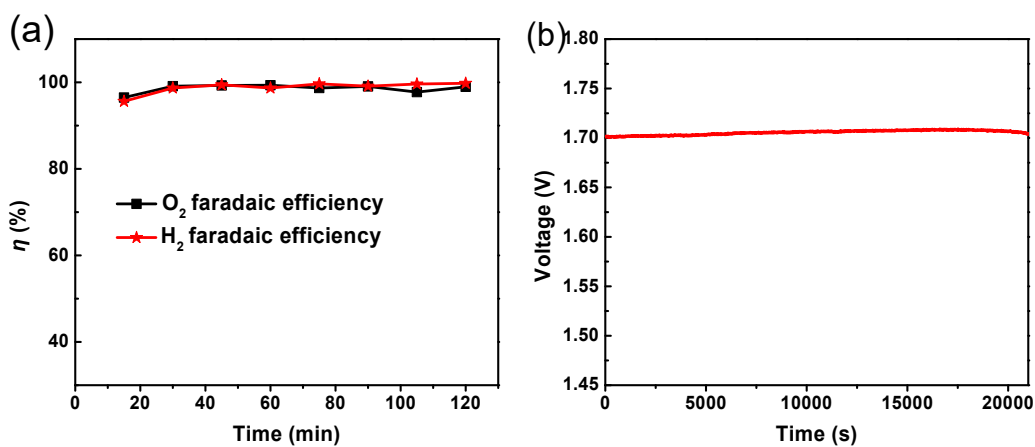


Fig. S18. (a) The faradaic efficiency of produced H₂ and O₂ during water splitting process. (b) Chronopotentiometry responses of Co_{0.85}Se/NC//Co_{0.85}Se/NC during water splitting process.

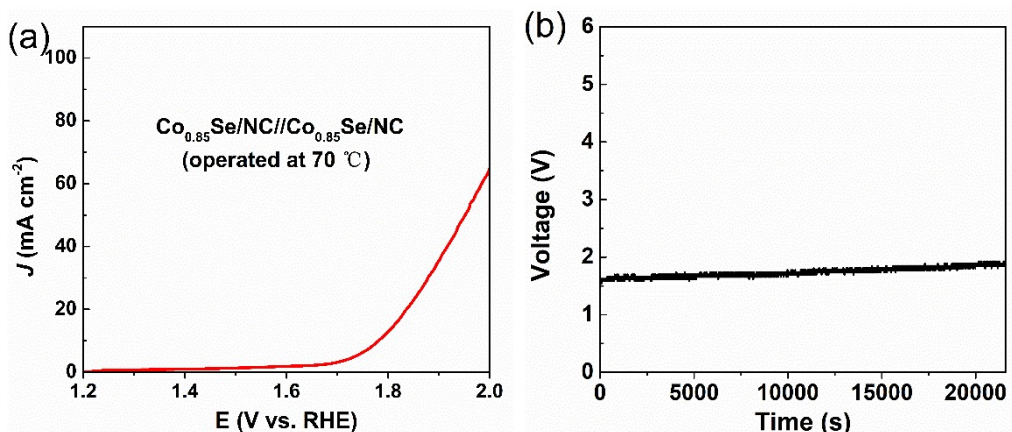


Fig. S19. (a) Polarization curves of $\text{Co}_{0.85}\text{Se}/\text{NC} // \text{Co}_{0.85}\text{Se}/\text{NC}$ cell in 1.0 M KOH electrolyte operated at 70 °C. (b) Chronopotentiometry responses of $\text{Co}_{0.85}\text{Se}/\text{NC} // \text{Co}_{0.85}\text{Se}/\text{NC}$ during water splitting process operated at 70 °C.

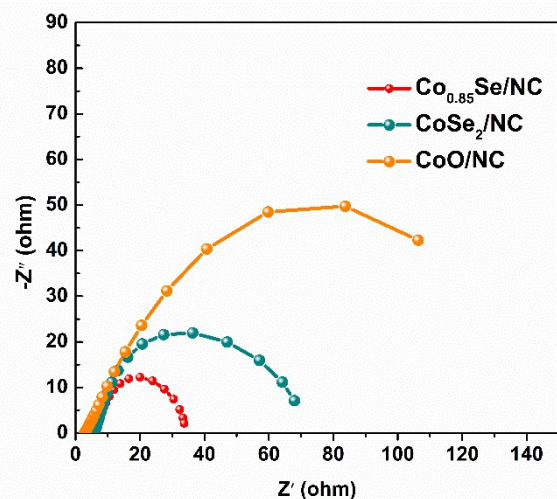


Fig. S20. Electrochemical impedance spectra of prepared catalyst-based ZABs.



Fig. S21. The photograph of the ZAB charged by a solar cell.

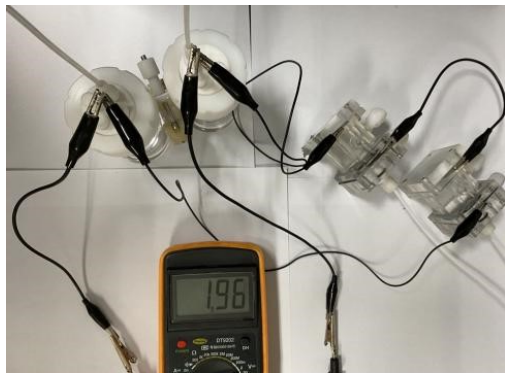


Fig. S22. The photographs of the overall water splitting device driven by ZABs.

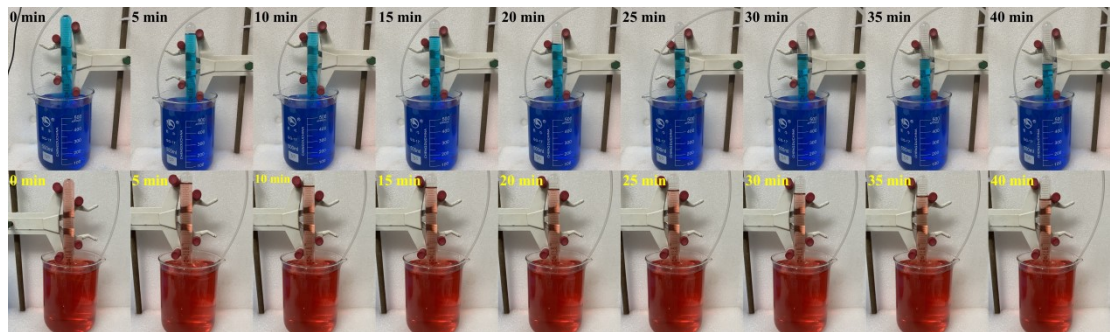


Fig. S23. The optical images of the gas collection tubes at fifteen-minute intervals over two-hour period during the overall water splitting process driven by ZABs.

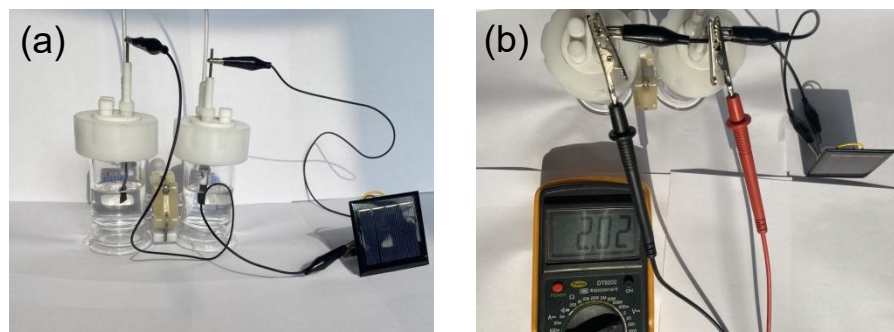


Fig. S24. Photographs of the overall water splitting device driven by a solar cell.

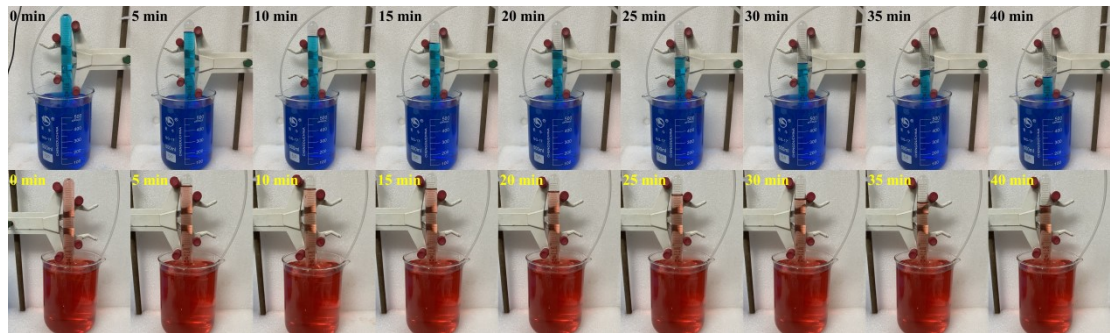


Fig. S25. The optical images of the gas collection tubes at fifteen-minute intervals over two-hour period during the overall water splitting process driven by a solar cell.

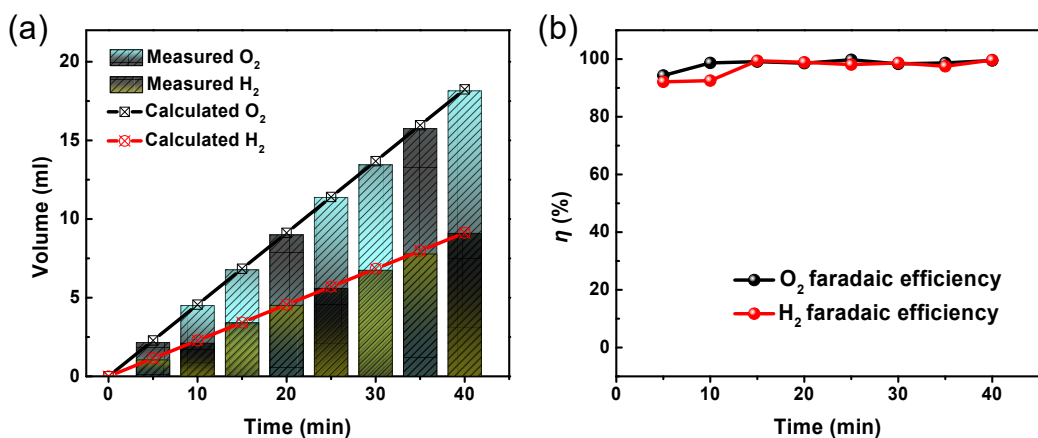


Fig. S26. (a) The corresponding measured and calculated gas volumes of H₂ and O₂ during water splitting process driven by a solar cell. (b) The faradaic efficiency of produced H₂ and O₂ during water splitting process driven by a solar cell.

Table S1. Comparison of the electrocatalytic activity of recently reported bifunctional Co-based electrocatalysts in alkaline electrolyte.

Catalyst	$E_{j=10}$ / (V vs. RHE)	E_{onset} / (V vs. RHE)	$E_{1/2}$ / (V vs. RHE)	E_{gap} / (V vs. RHE)	Ref.
Co _{0.85} Se/NC	1.505	0.901	0.797	0.708	This work.
Co ₉ S ₈ /Co	1.609	0.91	0.804	0.805	[3]
Co ₃ Mo ₃ N	1.52	0.85	0.75	0.77	[4]
Co-POP	1.57	N.A.	0.87	0.70	[5]
CoSP-850-10	1.59	N.A.	0.85	0.74	[6]
Co _{0.85} Se@C nanofibers	1.58	N.A.	0.82	0.76	[7]
Ag-CeO ₂ -Co ₃ O ₄	1.57	0.90.	0.80	0.77	[8]
Co-CoN ₄	1.54	0.91	0.83	0.71	[9]
Co/Ru SAs-N-C	1.568	N.A.	0.855	0.713	[10]
Co-N-C	1.459	N.A.	0.858	0.601	[11]
CoNi/NHCS-TUC-3	1.686	0.91	0.88	0.806	[12]
NiCo ₂ O ₄ /NLG	1.52	N.A.	0.85	0.67	[13]
CoNiP/PNC	1.7	0.90	0.84	0.86	[14]

Table S2. Comparison of the overall water splitting activity of recently reported transition metal-based electrocatalysts.

Catalyst	Substrate	$E_{j=10} / (\text{V vs. RHE})$	Ref.
Co _{0.85} Se/NC	Ni foam	1.70	This work.
FeNiP/NPCS	Ni foam	1.71	[15]
Ni-N-P	Ni foam	1.70	[16]
Co ₃ Mo ₃ N	Carbon cloth	1.65	[4]
FexNiy/CeO ₂	Ni foam	1.70	[17]
Co _{0.82} Ni _{0.18} P@NC	Ni foam	1.67	[18]
NiYSZ	Ni foam	1.70	[19]
Mo-CoP	Carbon paper	1.70	[20]
Co ₃ O ₄ @PPy	Ni foam	1.67	[21]

Table S3. The measured and calculated volumes of produced H₂ and O₂ during overall water splitting.

Times (min)	H ₂			O ₂		
	V _{measured} (ml)	V _{calculated} (ml)	η (%)	V _{measured} (ml)	V _{calculated} (ml)	η (%)
0	0	0	0	0	0	0
15	2.2	2.28	96.49	1.09	1.14	95.61
30	4.52	4.56	99.12	2.25	2.28	98.68
45	6.79	6.84	99.27	3.4	3.42	99.42
60	9.06	9.12	99.34	4.5	4.56	98.68
75	11.25	11.4	98.68	5.68	5.7	99.65
90	13.55	13.68	99.05	6.78	6.84	99.12
105	15.6	15.96	97.74	7.95	7.98	99.62
120	18.05	18.24	98.96	9.1	9.12	99.78

Table S4. The performance comparison of present reported rechargeable ZAB based on transition metal-based electrocatalysts.

Catalyst	Voltage gap (V)	Peak power density (mW cm ⁻²)	Cycling conditions and stability	Ref.
Co _{0.85} Se/NC	0.92 at 20 mA cm ⁻²	108	20 mA cm ⁻² , 40 min/cycle for 160 h, 4 h/cycle for 180 h, no obvious change	This work.
CoNi-NCNT	N.A.	88	10 mA cm ⁻² , 40 min/cycle for 150 cycles	[22]
Fe-Co ₄ N@N-C nanosheet array	0.80 at 10 mA cm ⁻²	105	5 mA cm ⁻² , 1 h/cycle for 1020 cycles, voltage gap increased ~0.1 V	[23]
Fe ₁ Zn ₃₀ NC _{PDI}	N.A.	86	10 mA cm ⁻² for 300 cycles	[24]
Cu@LSCNC _{0.05}	N.A.	136	10 mA cm ⁻² , 10 min/cycle for 500 cycles	[25]
FeN _x /CMCC	0.79 at 10 mA cm ⁻²	99.6	10 mA cm ⁻² , 2 h per cycle for 335 h	[26]
Ni ₃ Fe/N-C	0.79 at 10 mA cm ⁻²	N.A.	10 mA cm ⁻² , 4 h/cycle for 105 cycles; voltage gap increased ~0.20 V	[27]
Co@pNC	0.61 at 5 mA cm ⁻²	150.3	5 mA cm ⁻² , 10 min per cycle for 400cycles	[28]
Co-SA/N-C ₉₀₀	N.A.	191.11	10 mA cm ⁻² , 10 min/cycle for 585 cycles	[29]

Table S5. The measured and calculated volumes of produced H₂ and O₂ during overall water splitting driven by ZABs.

Times (min)	H ₂			O ₂		
	V _{measured} (ml)	V _{calculated} (ml)	η (%)	V _{measured} (ml)	V _{calculated} (ml)	η (%)
0	0	0	0	0	0	0
5	1.65	1.71	96.49	0.85	0.855	99.42
10	3.35	3.42	97.95	1.65	1.71	96.49
15	5.05	5.13	98.44	2.52	2.565	98.25
20	6.79	6.84	99.27	3.4	3.42	99.42
25	8.45	8.55	98.83	4.15	4.275	97.08
30	10.20	10.26	99.42	5.05	5.13	98.44
35	11.75	11.97	98.16	5.85	5.985	97.74
40	13.45	13.68	98.32	6.75	6.84	98.68

Table S6. Comparison of reported solar-to-hydrogen conversion efficiency.

Co _{0.85} Se/NC	4.34%	This work.
NiFeP	4.6%	[30]
IrCo	1.19%	[31]
CoP/NGQDsNCs	(AQE) 0.23%	[32]
RuO ₂ /Ti	3%	[33]
ZnO/Au	3.2%	[34]

Table S7. The measured and calculated volumes of produced H₂ and O₂ during water splitting driven by a solar cell.

Times (min)	V _{measured} (ml)	H ₂ V _{calculated} (ml)	η (%)	V _{measured} (ml)	O ₂ V _{calculated} (ml)	η (%)
0	0	0	0	0	0	0
5	2.15	2.28	94.30	1.05	1.14	92.11
10	4.5	4.56	98.68	2.11	2.28	92.54
15	6.78	6.84	99.12	3.4	3.42	99.42
20	8.99	9.12	98.57	4.51	4.56	98.90
25	11.37	11.4	99.74	5.59	5.7	98.07
30	13.45	13.68	98.32	6.75	6.84	98.68
35	15.75	15.96	98.68	7.78	7.98	97.49
40	18.15	18.24	99.51	9.09	9.12	99.67

The calculation of solar-to-ZAB efficiency:

$$\eta_{solar - ZAB} = \frac{\frac{E_{ZAB\ charge}}{E_{solar\ cell}}}{\frac{V * I * t}{S * P * t * EE_{solar\ cell}}} = \frac{2.0\ V * 9.63\ mA/cm^2 * 10^{-3} * 1\ cm^2}{0.0016\ m^2 * 1000\ W/m^2 * 20\%} * 100 = 6.02\%$$

V: charged voltage of ZAB

I: charged current density

t: reaction time

S: area (0.0016 m² in our work)

P: 1000 W m⁻² (the solar irradiation power density on earth at Air Mass 1.5 Global)

[35]

Supposing EE_{solar cell} = 20%

ZAB-to-water splitting efficiency:

$$\eta_{ZAB - water} = \frac{\frac{E_{water\ splitting}}{E_{ZAB\ discharge}}}{\frac{U * I * t}{V * I * t}} =$$

$$\frac{1.96 V * 45 mA * 10^{-3} * 1 cm^2 * 40 * 60 s}{1.10 V * 2 * 45 mA * 10^{-3} * 1 cm^2 * 40 * 60 s * 100} = 89.10\%$$

U: voltage of water splitting

I: current density of water splitting

ZAB-to-H₂ efficiency:

$$\eta_{ZAB - H_2} = \frac{\frac{E_{H_2}}{E_{solar cell}} \cdot standard molar enthalpy of combustion * n_{(H_2)}}{V * I * t}$$

$$= \frac{285 * 10^3 J/mol * 13.45 mL * 10^{-3} \div 22.4 L/mol}{1.10 V * 2 * 45 mA * 10^{-3} * 1 cm^2 * 40 * 60 s} * 100 =$$

72.02%

The E_{H_2} was calculated in terms of the standard molar enthalpy of combustion (-285 kJ/mol) [36].

Self-powered system efficiency (solar-to-water splitting device):

$$\eta = \eta_{solar - ZAB} * \eta_{ZAB - H_2} = 6.02\% * 72.02\% = 4.34\%$$

Solar-to-H₂ efficiency:

$$\eta = \eta_{solar - ZAB} * \eta_{ZAB - water} = 6.02\% * 89.10\% = 5.36\%$$

Direct solar-to-H₂ efficiency:

$$\eta = \frac{\frac{E_{H_2}}{E_{solar cell}} \cdot standard molar enthalpy of combustion * n_{(H_2)}}{P * t} =$$

$$= \frac{285 * 10^3 J/mol * 18.15 mL * 10^{-3} \div 22.4 L/mol}{0.0016 m^2 * 1000 W/m^2 * 40 * 60 s} * 100 = 6.01\%$$

References:

- [1] G. Chen, T. Wang, J. Zhang, P. Liu, H. Sun, X. Zhuang, M. Chen, X. Feng, *Adv. Mater.*, 2018, **30**, 1706279.
- [2] L. Wu, L. Yu, F. Zhang, B. McElhenny, D. Luo, A. Karim, S. Chen, Z. Ren, *Adv. Funct. Mater.*, 2021, **31**, 2006484.
- [3] K. Cui, Q. Wang, Z. Bian, G. Wang, Y. Xu, *Adv. Energy Mater.*, 2021, **11**, 2102062.
- [4] Y. Yuan, S. Adimi, T. Thomas, J. Wang, H. Guo, J. Chen, J. Attfield, F. J. DiSalvo, M. Yang, *Innovation*, 2021, **2**, 100096.
- [5] H. Lei, Q. Zhang, Z. Liang, H. Guo, Y. Wang, H. Lv, X. Li, W. Zhang, U. Apfel, R. Cao, *Angew. Chem. Int. Ed.*, 2022, **61**, e2022011.
- [6] Y. Wang, K. Wang, J. Yu, Y. Ma, X. Yang, H. Jiang, Y. Liu, J. Li, W. Li, *J. Power Sources*, 2021, 482, 228897.
- [7] L. Gui, Z. Huang, D. Ai, B. He, W. Zhou, J. Sun, J. Xu, Q. Wang, L. Zhao, *Chem. Eur. J.*, 2020, **26**, 4063-4069.
- [8] T. Li, Z. H. X. Li, M. Jiang, Q. Liao, R. Ding, S. Liu, C. Zhao, W. Guo, S. Zhang, H. He, *Surf. Interfaces*, 2022, **33**, 102270.
- [9] K. Ding, J. Hu, J. Luo, L. Zhao, W. Jin, Y. Liu, Z. Wu, G. Zou, H. Hou, X. Ji, *Adv. Funct. Mater.*, 2022, **32**, 2207331.
- [10] L. Zhang, J. Yao, J. Zhang, W. He, Y. Li, L. Liang, C. Liu, H. Liu, *Catal. Sci. Technol.*, 2022, **12**, 5435-5441.
- [11] H.J. Son, M. J. Kim, S.H. Ahn, *Chem. Eng. J.*, 2021, **414**, 128739.
- [12] K. Sheng, Q. Yi, A.L. Chen, Y. Wang, Y. Yan, H. Nie, X. Zhou, *ACS Appl. Mater. Inter.*, 2021, **13** 45394-45405.
- [13] W. Zhong, X. Zhao, J. Qin, J. Yang, *Chinese J. Chem.*, 2020, **39**, 655-660.
- [14] W. Sun, Y. Xu, P. Yin, Z. Yang, *Appl. Surf. Sci.*, 2021, **554**, 149670.
- [15] J.-T. Ren, Y.-S. Wang, L. Chen, L.-J.Gao, W.-W. Tian, Z.-Y. Yuan, *Chem. Eng. J.*, 2020, **389**, 124408.
- [16] S. Zhang, X. Zhang, H. Zhu, H. Xing, J. Li, E. Wang, *Electrochim. Commun.*, 2020, **114**, 106701.
- [17] L. Chen, H. Jang, M. G. Kim, Q. Qin, X. Liu, J. Cho, *Inorg. Chem. Front.*, 2020, **7**, 470-476.
- [18] T. Xie, B. Wang, S. Yang, Q. Xu, X. Cheng, C. Zhou, J. Hu, *J. Alloys Compd.*, 2022, **621**, 166111.

- [19] S. Sivakumar, S. Yugeswaran, K. V. Sankar, L. Kumaresan, G. Shanmugavelayutham, Y. Tsur, J. Zhu, *J. Power Sources*, 2020, **473**, 228526.
- [20] L. Li, Y. Guo, X. Wang, X. Liu, Y. Lu, *Langmuir* 2021, **37**, 5986-5992.
- [21] Y. Tong, H. Liu, M. Dai, L. Xiao, X. Wu, *Chinese Chem. Lett.*, 2020, **31**, 2295-2299.
- [22] M. Qiao, Y. Wang, T. Wågberg, X. Mamat, X. Hu, G. Zou, G. Hu, *J. Energy Chem.*, 2020, **47**, 146-154.
- [23] J. Yu, B.Q. Li, C.X. Zhao, J.N. Liu, Q. Zhang, *Adv. Mater.*, 2020, **32**, e1908488.
- [24] J. Shen, Q. Liu, Q. Sun, J. Ren, X. Liu, Z. Xiao, C. Xing, Y. Zhang, G. Yang, Y. Chen, *J. Ind. Eng. Chem.*, 2023, **118**, 170-180.
- [25] X. Ou, Q. Liu, F. Wei, C. Sun, Y. Liao, Y. Zhou, F. Yan, *Chem. Eng. J.*, 2023, **451**, 139037.
- [26] Q. Zhou, Z. Yao, X. Zeng, N. Wei, S. Zhang, C. Xiong, *Mater. Today Chem.*, 2022, **24**, 100844.
- [27] Y. Niu, X. Teng, S. Gong, Z. Chen, *J. Mater. Chem. A*, 2020, **8** 13725-13734.
- [28] M. Shen, X. Lin, W. Xi, X. Yin, B. Gao, L. He, Y. Zheng, B. Lin, *J. Colloid Interf. Sci.*, 2023, **633**, 374-382.
- [29] N. Li, L. Li, J. Xia, M. Arif, Sh. Zhou, F. Yin, G. He, H. Chen, *J. Mate. Sci. Technol.*, 2023, **10**, 224-231.
- [30] R. Yang, X. Zheng, M. Qin, B. Lin, X. Shi, Y. Wang, *Adv. Sci.*, 2022, 2201594.
- [31] D. D. Babu, Y. Huang, G. Anandhababu, X. Wang, R. Si, M. Wu, Q. Li, Y. Wang, J. Yao, *J. Mater. Chem. A*, 2019, **7**, 8376-8383.
- [32] Z. Zhong, J. Liu, X. Xu, A. Cao, Z. Tao, W. You, L. Kang, *J. Mater. Chem. A*, 2021, **9**, 2404-2413.
- [33] S. Esiner, J. Wang, R. Janssen, *Cell Rep. Phys. Sci.*, 2020, **1**, 100058.
- [34] Y. Wang, W. Wang, J. Fu, Y. Liang, L. Yao, T. Zhu, *Renewable Energy*, 2021, **168**, 647-658.
- [35] J. Qi, W. Zhang, R. Cao, *Adv. Energy Mater.*, 2018, **8**, 1701620.
- [36] J. Li, D. Chu, D. R. Baker, A. Leff, P. Zheng, R. Jiang, *ACS Appl. Energy Mater.*, 2021, **4**, 9969-9981.